Deuteron NMR study of a long-chain smectic liquid crystal: Molecular order and dynamics

Ronald Y. Dong
Department of Physics and Astronomy, Brandon University, Brandon, Manitoba, Canada R7A 6A9
and Department of Physics and Astronomy, University of Manitoba, Winnipeg, Manitoba, Canada R3T 2N2
(Received 9 July 1999)

Deuteron Zeeman (T_{1Z}) and quadrupolar (T_{1Q}) spin-lattice relaxation times and quadrupolar splittings were measured in the nematic and smectic *A* phases of a chain-deuterated 4-*n*-octyloxy-4'-cyanobiphenyl (8OCB-d_{17}) at 15.1 and 46 MHz. To model the NMR observables, the so-called pentane effect is used to limit the number of possible conformations in the chain, and is found to be a good approximation. The additive potential method is employed to construct the potential of mean torque using the quadrupolar splittings. A decoupled model is used to describe correlated internal motions in the chain, which are independent of the molecular reorientation. The latter motion is treated using the small-step rotational diffusion model of Nordio (Tarroni and Zannoni), while the former motion is described using a master rate equation. In the nematic phase, order director fluctuations are found to be necessary. The relaxation data in both mesophases were treated using a global target method, and the derived motional parameters are acceptable in comparison with those found for 6OCB. [S1063-651X(99)11711-2]

PACS number(s): 61.30.Eb, 33.25.+k

I. INTRODUCTION

It is well known that NMR spectroscopy, including ^{2}H-NMR, has been proven useful in elucidating the structure, molecular order, and dynamics of liquid crystalline materials [1]. In particular, from chemical studies many physical properties such as the order parameter, the nematic-isotropic transition temperature, the transition entropy, and the splay elastic constant are found [2] to be profoundly influenced by the lengths of alkyl(oxy) chains in liquid crystals. As a result, there are increasing numbers [3–10] of ^{2}H-NMR relaxation studies aiming to probe the dynamics of liquid crystal molecules with increasing chain lengths. Simultaneously theoretical models [11–13] are proposed to account for the internal chain mobility of molecules moving in an anisotropic medium. The present study focuses on extending the chain lengths of flexible molecules previously studied to one that contains nine atoms in the chain backbone. The chosen molecule is a chain-deuterated smectogen 4-n-octyloxy-d_{17}-4′-cyanobiphenyl (8OCB-d_{17}) which shows nematic (*N*) and smectic *A* (Sm*A*) phases upon decreasing the temperature.

There are many relaxation mechanisms responsible for relaxing the nuclear spin in liquid crystals. As the dominant spin interaction for deuterons ($I=1$) is the nuclear quadrupolar interaction, only intramolecular relaxation mechanisms need to be considered. Besides the molecular reorientation and internal bond rotations which relax the deuteron spin as in ordinary liquids, there is a unique mechanism in liquid crystals known as order director fluctuations (ODF's) [14–18]. These fluctuations involve collective motions of a large number of molecules with respect to the equilibrium director $\hat{n}_o$. The first variable frequency T_1 study [19] indicated that the usual Lorentzian frequency dependence expected by the BBP theory [20] for ordinary liquids was not observed. It is now well established that the spin-lattice relaxation rate due to ODF's obeys a $\omega^{-1/2}$ frequency relation as predicted by Pincus [14]. Furthermore, in a small angle (θ) approximation, where θ is the angle between the instantaneous director $\hat{n}$ and its equilibrium orientation ($\hat{n}_o$), ODF's contribute only to the spectral density $J_1(\omega)$ and make zero contributions to $J_2(2\omega)$ and $J_0(\omega)$. Here we will ignore any higher order ODF contributions to $J_0(\omega)$ and $J_2(2\omega)$ [17,18], and the small negative cross-term [21] between ODF's and molecular reorientation.

The reorientation of molecules in liquid crystals can be described by the rotational diffusion model [22,23]. The model assumes a stochastic Markov process for molecular reorientations in which each molecule moves in time as a sequence of small angular steps caused by collisions with its surrounding molecules and under the influence of a potential of mean torque set up by those molecules. Nordio and coworkers [23] considered reorientations of cylindrical rigid molecules in uniaxial phases (*N*, Sm*A*). Each molecule is characterized by a rotational diffusion tensor whose principal elements ($D_{xx}=D_{yy}=D_\perp, D_{zz}=D_\parallel$) are defined in a frame fixed on the molecule. A number of motional models of increasing complexity has been proposed [24–28] including the general case of a biaxial molecule moving in a biaxial phase. Of relevance to the present study is the Tarroni-Zannoni model [26] which uses $D_{xx}\neq D_{yy}\neq D_{zz}$ and a potential of mean torque with a nonzero molecular biaxiality. When dealing with molecules with internal degrees of freedom, the number of different conformers in the chain of the molecule can be generated using the rotameric state (RIS) model of Flory [29]. It is customary to treat molecular dynamics of flexible molecules using a decoupled model [11–13], in which conformational transitions within the chain(s) are assumed not to depend on the reorientation of the entire molecule. The rotational diffusion tensor is assumed to be the one for an ''average'' conformer. In other words, the diffusion tensors for different conformers do not deviate substantially from each other. Furthermore, correlated internal bond rotations in the chain are dealt with an extension of the

RIS model to the time domain by means of a master rate equation [13]. The dimension of the rate matrix is governed by the number of available configurations, and therefore increases rapidly with an increasing number of atoms in the chain. Although this should, in principle, not be a problem, in practice the computation time required to fit the relaxation data can become unmanageable. In the present study of 8OCB, the number of configurations is reduced to 577 by imposing the pentane effect, i.e., the energy $E_{g^{\pm}g^{\mp}}$ for forming a $g^{+}g^{-}$ or $g^{-}g^{+}$ linkage in the carbon-carbon backbone is assumed to be infinitely large. Indeed, in proposing the decoupled model [12,13,30] for the 5CB molecule a diamond lattice for the C-C backbone was employed in which without the pentane effect two atoms would occupy the same lattice site. Later, we found that the essential physics of molecular motions on spin relaxation was not drastically altered by using a more realistic geometry and removing the pentane effect in 5CB [31]. Thus the use of pentane effect to limit the number of configurations in 8OCB should be a reasonable approximation. The paper is organized as follows. Section II outlines the basic theory used to analyze the quadrupolar splittings and the spectral density data. Section III contains a brief description of the experimental method, while Sec. IV contains results and discussion. In particular, a global target approach [32] is used to analyze the relaxation data from both the nematic and smectic A phases and both Larmor frequencies. This approach has been shown [8–10,33] to give more reliable NMR dynamical parameters. In particular, the approach should be used [34] when the model parameters may be highly correlated and/or affected by large statistical errors.

II. BASIC THEORY

The evolution of a spin system is governed by a spin Hamiltonian which contains time fluctuating terms as a result of thermal motions (both reorientational and collective modes) of liquid-crystal molecules. From the standard spin relaxation theory [35] for deuterons ($I=1$), the Zeeman and quadrupolar spin-lattice relaxation rates are given in terms of spectral densities $J_m(m\omega)$ by

$$T_{1Z}^{-1}=J_1(\omega_o)+4J_2(2\omega_o),$$
$$T_{1Q}^{-1}=3J_1(\omega_o), \tag{1}$$

where $\omega_o/2\pi$ is the Larmor frequency. The spectral density is simply the Fourier transform of the autocorrelation function $G_m(t)$,

$$J_m(m\omega)=\frac{3\pi^2}{2}(q_{\mathrm{CD}})^2\int_0^{\infty}G_m(t)\cos(m\omega t)dt, \tag{2}$$

where $q_{\mathrm{CD}}=e^2qQ/h$ is the quadrupolar coupling constant, and $G_m(t)$ may be expressed in terms of the Wigner rotation matrix $D_{mn}^2(\Omega)$ in the fluctuating Hamiltonian

$$G_m(t)=\langle D_{m0}^2(\Omega_{LQ}(0))D_{m0}^{2*}(\Omega_{LQ}(t))\rangle, \tag{3}$$

where the angle brackets denote an ensemble average and the Euler angles $\Omega_{LQ}(t)$ specify the orientation of the principal axes of the electric-field-gradient (EFG) tensor (the asymmetry parameter η is set to zero) with respect to the laboratory frame whose z_L axis is defined by the external magnetic field. To evaluate $G_m(t)$, one needs to transform the EFG tensor through successive coordinates [1] to account for internal rotations and molecular reorientations, as well as collective motions when applicable. These different motional processes occur over sufficiently different time scales such that small couplings among them can often be neglected. Here we only write down the necessary formulas for these motions to calculate their corresponding theoretical spectral densities.

It is generally accepted that a second rank potential of mean torque $U(\Omega)$ can be used to solve the rotational diffusion problem of a rigid rodlike molecule. For uniaxial phases, the orientating potential is independent of the Euler angle α, and $U(\Omega)$ can be parametrized by two second rank coefficients a_{20} and a_{22},

$$\frac{U(\beta,\gamma)}{k_BT}=a_{20}\left(\frac{3}{2}\cos^2\beta-\frac{1}{2}\right)+a_{22}\sqrt{\frac{3}{2}}\sin^2\beta\cos 2\gamma, \tag{4}$$

where $a_{2-2}=a_{22}$ is used, and k_B is the Boltzmann's constant. The moleuclar biaxial parameter $\xi=a_{22}/a_{20}$ is a measure of the deviation from cylindrical symmetry of a molecule. When a_{22} is set to zero as in the model of Nordio and co-workers, the orienting potential is identical to the Maier-Saupe potential. In principle, the coefficients a_{20} and a_{22} can be determined from a knowledge of order parameters $S_{zz}(\langle P_2\rangle)$ and $S_{xx}-S_{yy}$. For flexible molecules forming uniaxial mesophases, the orienting potential is first established from the order tensor of an ''average'' conformer (see below). For the deuterons in the chain, the decoupled model [13] is used to describe correlated internal rotations in the octyloxy chain, and the model of Nordio and co-workers with $a_{22}\neq 0$ is used [26] to account for rotational diffusions of the molecule. Using the notation given in Ref. [26] for molecular reorientations, the spectral densities $J_{mR}^{(i)}(m\omega)$ for the deuterons on the C_i carbon of the chain are given by ($m\neq 0$)

$$J_{mR}^{(i)}(m\omega)=\frac{3\pi^2}{2}(q_{\mathrm{CD}}^{(i)})^2\sum_n\sum_{n'}\sum_{k=1}^{577}\left(\sum_{l=1}^{577}d_{n,0}^2(\beta_{M,Q}^{(i)l})x\exp[-in\alpha_{M,Q}^{(i)l}]x_l^{(1)}x_l^{(k)}\right)$$
$$\times\left(\sum_{l'=1}^{577}d_{n',0}^2(\beta_{M,Q}^{(i)l'})\exp[-in'\alpha_{M,Q}^{(i)l'}]x_{l'}^{(1)}x_{l'}^{(k)}\right)\sum_j\frac{(\beta_{mnn'}^2)_j[(\alpha_{mnn'}^2)_j+|\lambda_k|]}{m^2\omega^2+[(\alpha_{mnn'}^2)_j+|\lambda_k|]^2}, \tag{5}$$

where $q_{\mathrm{CD}}^{(i)}=165$ kHz, $\beta_{M,Q}^{(i)l}$ and $\alpha_{M,Q}^{(i)l}$ are the two polar angles for the C_i-D bond of the conformer l in the molecular frame attached to the biphenyl core, and λ_k and $\vec{x}^{(k)}$ are the eigenvalues and eigenvectors from diagonalizing a symmetrized transition rate matrix. The rate matrix describing conformational changes in the octyloxy chain contains jump constants k_1, k_2, and k_3 for one-, two-, and three-bond motions [1] in the chain. For 8OCB, the O-C_α bond is taken to be fixed on the phenyl ring plane with a COC_α angle of 126.4° [36]. Using the pentane effect to eliminate any conformer which contains either a g^+g^- or g^-g^+ group in the chain, the rate matrix has the dimensions of 577×577.

The effect of chain flexibility on the ODF contribution to the spectral density has been discussed previously [37] by us. In the small θ approximation, for the ith deuterons one obtains

$$J_{IDF}^{(i)}(\omega)=\frac{3\pi^2}{2}(q_{\mathrm{CD}}^{(i)})^2\frac{A(1-4\alpha)}{(1-3\alpha)^2}(S_{\mathrm{CD}}^{(i)})^2\Im(\omega_c/\omega)/\sqrt{\omega}, \tag{6}$$

where the cutoff function $\Im(\omega_c/\omega)$ is given [21] by

$$\Im(x)=\frac{1}{2\pi}\ln\left[\frac{x-\sqrt{2x}+1}{x+\sqrt{2x}+1}\right]+\frac{1}{\pi}[\tan^{-1}(\sqrt{2x}-1)+\tan^{-1}(\sqrt{2x}+1)], \tag{7}$$

and the high-frequency cutoff $\omega_c=4\pi^2K/\eta\lambda_C^2$, with K being the average elastic constant and η the average viscosity, and the parameter $\alpha=k_BT/K\lambda_C$ is a measure of the magnitude of ODF with λ_C, the cutoff wavelength, being typically the order of the molecular length. The segmental order parameter of the C-D bond ($S_{\mathrm{CD}}^{(i)}$) at the ith carbon site is directly related to the quadrupolar splitting $\Delta\nu_i$ according to the relation

$$\Delta\nu_i=\tfrac{3}{2}q_{\mathrm{CD}}^{(i)}S_{\mathrm{CD}}^{(i)}. \tag{8}$$

It is noted that the director $\hat{n}_o$ is aligned along the external $\vec{B}$ field since 8OCB has a positive diamagnetic susceptibility anisotropy ($\Delta\chi>0$). The calculated spectral densities for the ith deuterons are now given by

$$J_1^{(i)}(\omega)=J_{1R}^{(i)}(\omega)+J_{1DF}^{(i)}(\omega), \tag{9}$$

$$J_2^{(i)}(2\omega)=J_{2R}^{(i)}(2\omega) \tag{10}$$

under the above-mentioned assumptions.

The additive potential (AP) method [38] is used to construct the external potential $U_{\mathrm{ext}}(n,\Omega)$ for each rigid conformer n in the potential of mean torque $U(n,\Omega)$,

$$U(n,\Omega)=U_{\mathrm{int}}(n)+U_{\mathrm{ext}}(n,\Omega), \tag{11}$$

where the internal energy $U_{\mathrm{int}}(n)$ is independent of the orientation of the director in a molecular frame fixed on the conformer n, and is given by the number (N_g) of *gauche* linkages,

$$U_{\mathrm{int}}(n)=N_gE_{tg}, \tag{12}$$

where E_{tg} is the energy difference between a *gauche* state in comparison with a *trans* state in the chain. The E_{tg}(OCC) is higher than the E_{tg}(CCC) due to the presence of an alkyloxy chain. To construct $U_{\mathrm{ext}}(n,\Omega)$ for the conformer n, one needs to know the geometry of the chain. The CCC, CCH, and HCH angles are assumed [39] to be 113.5°, 107.5°, and 113.6°, respectively. The O-C bond is taken to be identical to a C-C bond, and the OCC angle is set the same as a CCC angle. The dihedral angles ($\phi=0,\pm112°$) are for rotation about each C-C bond and also about the O-C bond in the octyloxy chain. The C_{ar}-O bond is included with the biphenyl core when calculating its interaction energy. Both the interaction tensors for the core and for each C-C bond are assumed to be cylindrically symmetric, and characterized by the parameters X_a and X_{cc}, respectively. Now the segmental order parameter $S_{\mathrm{CD}}^{(i)}$ is a weighted average of the segmental order parameter $S_{bb}^{n,i}$ for the C_i-D bond of the molecule having the conformer n,

$$S_{\mathrm{CD}}^{(i)}=\sum_n P_{\mathrm{eq}}(n)S_{bb}^{n,i} \tag{13}$$

where the b axis of the principal axis (a,b,c) frame of the nuclear quadrupolar interaction is taken to be along the methylene C-D bond ($\eta=0$), and the equilibrium $P_{\mathrm{eq}}(n)$ probability is given by

$$P_{\mathrm{eq}}(n)=\frac{1}{Z}\exp[-U_{\mathrm{int}}(n)/k_BT]Q_n, \tag{14}$$

with Z, the conformation-orientational partition, given by

$$Z=\sum_n \exp[-U_{\mathrm{int}}(n)/k_BT]Q_n, \tag{15}$$

and Q_n, the orientational partition function of the conformer n, given by

$$Q_n=\int \exp[-U_{\mathrm{ext}}(n,\Omega)/k_BT]d\Omega. \tag{16}$$

In the principal frame of $U_{\mathrm{ext}}(n,\Omega)$, one can easily calculate [40] the principal components $S_{\alpha\alpha}^n$ of the order matrix for the conformer n, from which one can obtain

$$S_{bb}^{n,i}=\sum_\alpha^{x,y,z} S_{\alpha\alpha}^n\cos^2\theta_{\alpha b}^{n,i} \tag{17}$$

where $\theta_{\alpha b}^{n,i}$ denote angles between the C_i-D bond (b axis) and a principal α axis. By modeling the segmental order profile at each temperature, the interaction parameters X_a and X_{cc} used in $U_{\mathrm{ext}}(n,\Omega)$ can be determined. Simultaneously the order parameter tensor for an ''average'' conformer of the molecule can be evaluated [1].

III. EXPERIMENTAL METHOD

The chain-deuterated (8OCB-d_{17}) was purchased from Merck, Sharp & Dohme (Montreal), and has the following

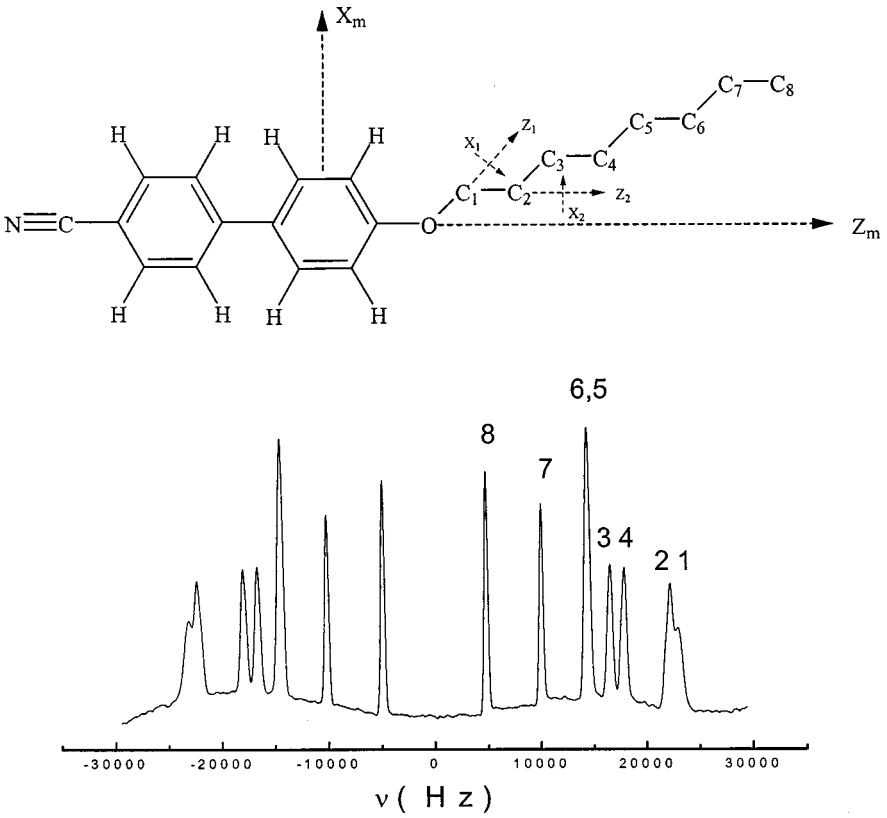

FIG. 1. A typical deuteron NMR spectrum of 8OCB-d_{17} showing the peak assignment, together with a 8OCB molecule showing various coordinate systems used in the text.

phase transition temperatures: Sm*A* to *N* at 339K and *N* to *I* at 352 K. The 8OCB molecule is schematically shown in Fig. 1(a) and the peak assignment of a representative spectrum of 8OCB-d_{17} is shown in Fig. 1(b). The assignments to C_3 and C_4 deuterons follow those obtained experimentally in 6OCB [41]. This seems to be consistent with our measured spin-lattice relaxation times at these carbon sites. Care was taken to ensure that spectral resolution was not degraded by using too large a sample to gain better signal-to-noise ratio. Indeed the peaks from C_1 and C_2, and those from C_5 and C_6, do overlap, but deconvolution of the peaks for the individual carbon's deuterons was carried out whenever possible, noting the proper lineshape of a coupled deuteron pairs [42]. This allowed separate determination of relaxation times for the carbon sites in question. At 15.1 MHz, peaks 1 and 2 could not be resolved by deconvolution at low temperatures, and the DMR signals of these carbon sites for relaxation measurements were obtained by simply integrating the areas in different parts of the overlapped (broad) line.

A home-built superheterodyne coherent pulse NMR spectrometer was operated for deuterons at 15.1 MHz using a Varian 15-in. electromagnet and at 46.05 MHz using a 7.1-T Oxford superconducting magnet. The sample was placed in an NMR probe whose temperature was regulated either by an external oil bath circulator or by an air flow with a Bruker BST-1000 temperature controller. The temperature gradient across the sample was estimated to be better than 0.3° C. The $\pi/2$ pulse width of about 4 μs was produced by an ENI power amplifier. Pulse control and signal collection were performed by a GE 1280 minicomputer. Fourier transform and data processing were done by Spectral Calc and Micro Origin softwares on a Pentium-PC computer. A broadband J-B (Wimperis) sequence [43] was used to simultaneously measure the Zeeman (T_{1Z}) and the quadrupole (T_{1Q}) spin-lattice relaxation times. The pulse sequence [1] was modified using an additional monitoring $\pi/4$ pulse to minimize any long-term instability of the spectrometer. This pulse was phase cycled to have a net effect of subtracting the signal from the J-B sequence the equilibrium magnetization. This has the added advantage of monitoring the sum $S(t)$ and the difference $D(t)$ of the component areas of the quadrupolar doublet according to

$$S(t) \propto \exp(-t/T_{1Z}),$$

$$D(t) \propto \exp(-t/T_{1Q}).$$

Signal collection was started 10 μs after each monitoring $\pi/4$ pulse, and averaged over 4096 scans at 46 MHz and up to 8192 scans at 15.1 MHz. The quadrupolar splittings were determined from a spectrum obtained by Fourier transforming the free induction decay signal after a $\pi/2$ pulse.

IV. RESULTS AND DISCUSSION

Figure 2 shows the experimental segmental order parameter $S_{CD}^{(i)}$ as a function of temperature in the N and Sm*A* phases of 8OCB-d_{17}. Equations (13)–(17) are used in our mean field calculations of the segmental order profiles at different temperatures. An optimization routine (AMOEBA) was used [44] to minimize the sum squared error f in fitting the experimental $S_{CD}^{(i)}$,

$$f = \sum_i \left(|S_{CD}^{(i)}| - |S_{CD}^{(i)\mathrm{Calc}}|\right)^2, \tag{18}$$

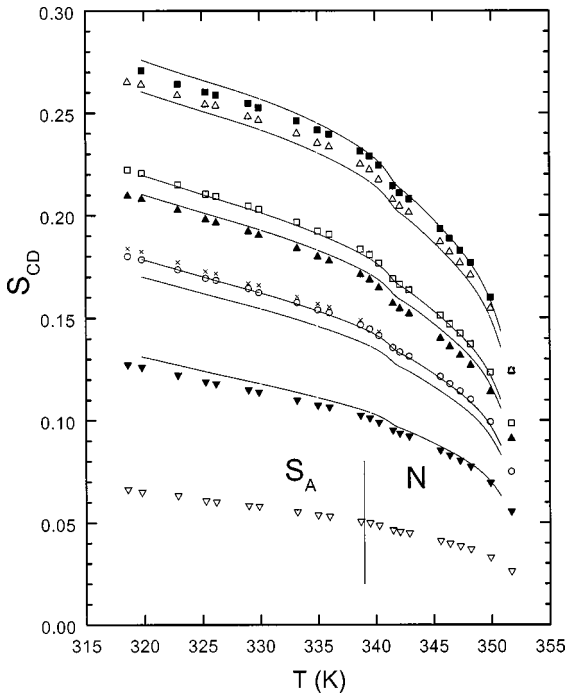

FIG. 2. Plot of segmental order parameters vs the temperature. The solid square, up triangle, ×, and down triangle denote C_1, C_3, C_5, and C_7 sites, respectively. The open up triangle, square, circle, and down triangle denote C_2, C_4, C_6, and C_8 sites, respectively, except in the *N* phase, where the circle is for both C_5 and C_6. The solid curves are the theoretical calculations for C_1–C_7 starting from the top. Note that the experimental splittings of C_3 and C_4 are reversed from those predicted by the theory.

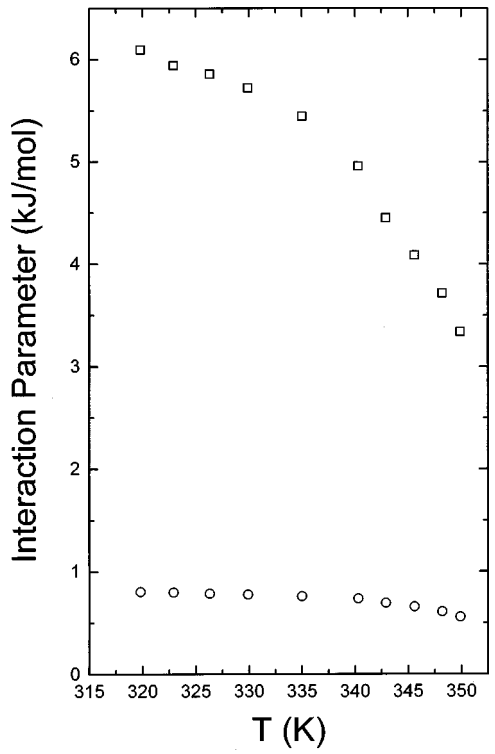

FIG. 3. Plot of interaction parameters X_a (square) and X_{cc} (circle) versus the temperature.

where the sum over *i* includes only the methylene deuterons in C_1 to C_7. The *f* values at different temperatures are of the order of 10^{-3}. The calculated segmental order parameters are indicated in Fig. 2 as solid lines. The tentative assignment of $\Delta\nu_3 < \Delta\nu_4$ cannot be reproduced by the AP method as seen in this figure. This was found previously in mean field calculations for 6OCB [9,36]. In working out $U_{\rm int}(n)$, we set $E_{tg}(\mathrm{CCC}) = 4000$ J/mol and $E_{tg}(\mathrm{OCC}) = 5600$ J/mol. These E_{tg} values are slightly higher than those used in 6OCB, while the derived interaction parameters X_a and X_{cc} versus the temperature in Fig. 3 are comparable to those found in 6OCB [9]. The interaction parameters found from fitting the quadrupolar splittings are used to find $P_{\rm eq}(n)$ needed for calculating the autocorrelation functions for internal motions in the chain. Furthermore, the order matrix of an ''average'' conformer of 8OCB has been evaluated at each temperature. Figure 4 shows its principal elements $\langle P_2\rangle$ and $\langle S_{xx}-S_{yy}\rangle$ as a function of temperature, from these the coefficients a_{20} and a_{22} in Eq. (4) are obtained. Despite the obvious deviations between calculated and observed segmental order parameters in Fig. 2, the resulting $P_{\rm eq}(n)$, a_{20}, and a_{22} are quite satisfactory for treating our relaxation data below.

The spectral density $J_1(\omega)$ and $J_2(2\omega)$ data versus the temperature for all the chain deuterons are shown in Fig. 5 at 15.1 and 46 MHz. It is clear from this figure that $J_1^{(i)}(\omega)$ show substantial frequency dependences at all carbon sites, while $J_2^{(i)}(2\omega)$ shows less frequency dependences. In our previous study of 6OCB [9], similar frequency behaviors of the spectral density data in its nematic phase were accounted only by the relatively ''slow'' molecular reorientation. Here we will see that ''slow'' molecular reorientations can describe the frequency dependences of $J_1^{(i)}(\omega)$ and $J_2^{(i)}(2\omega)$ in the Sm*A* phase, while some ODF contributions appear to be

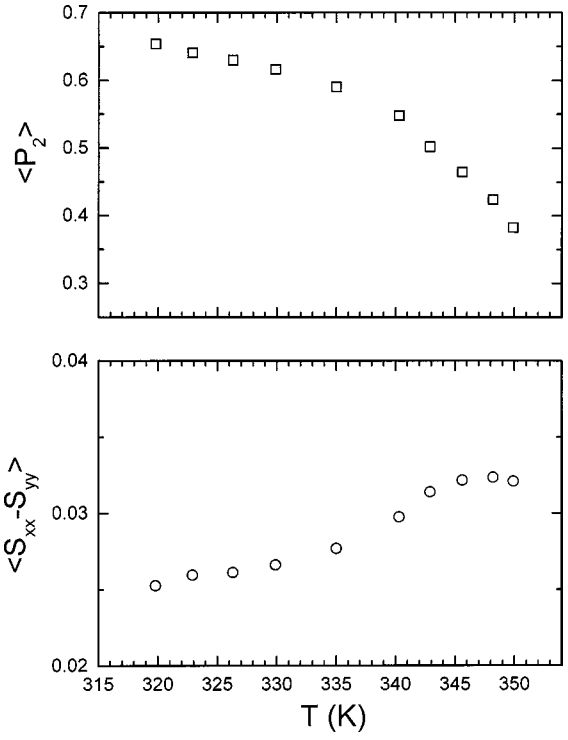

FIG. 4. Plots of the order parameters $\langle P_2\rangle$ and $\langle S_{xx}-S_{yy}\rangle$ of an ''average'' conformer of 8OCB as a function of temperature.

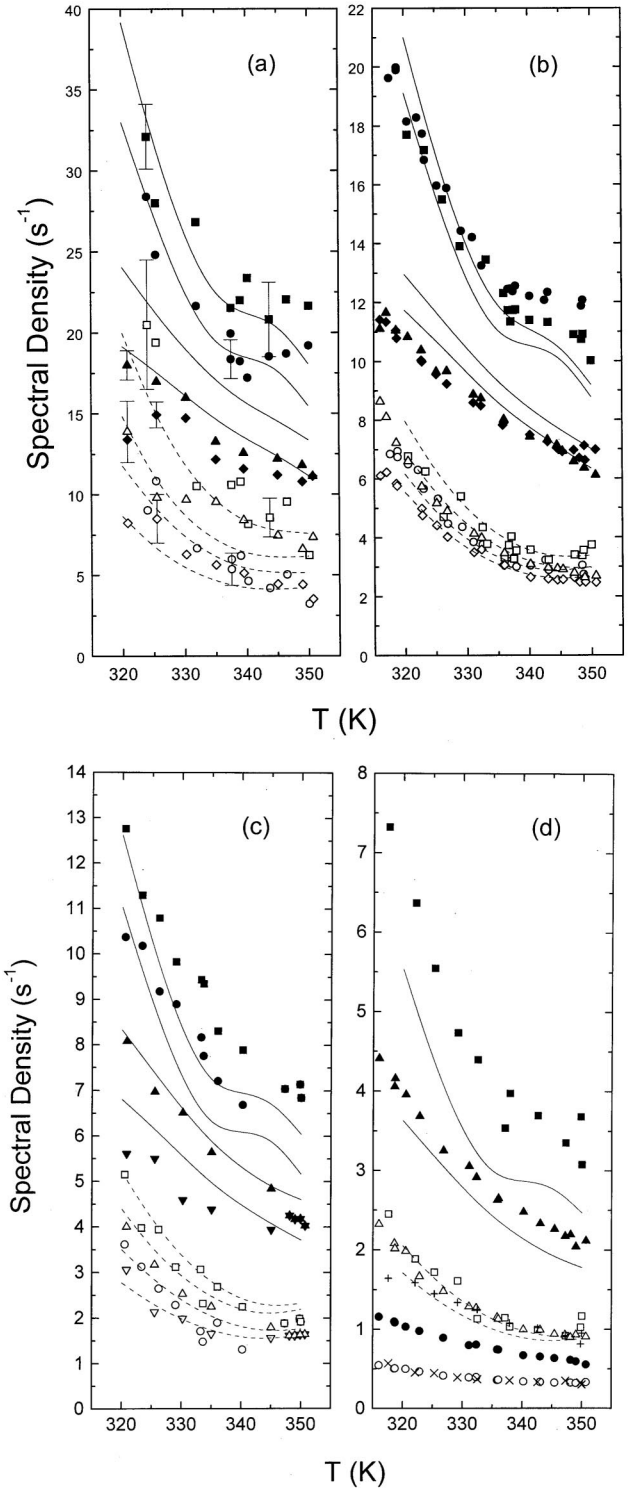

FIG. 5. Plots of spectral densities vs temperature in 8OCB. Closed symbols denote $J_1^{(i)}(\omega)$, and open symbols denote their corresponding $J_2^{(i)}(2\omega)$. (a) The square and circle are for C_1 and C_2 at 15.1 MHz, and the triangle and diamond are for C_1 and C_2 at 46 MHz. (b) The square and circle are for C_3 and C_4 at 15.1 MHz, and the triangle and diamond are for C_3 and C_4 at 46 MHz. (c) The square and circle are for C_5 and C_6 at 15.1 MHz, and the up triangle and down triangle are for C_5 and C_6 at 46 MHz. (d) The square and triangle are for C_7 at 15.1 and 46 MHz, respectively. For C_8, + and $\times$ denote $J_1^{(i)}(\omega)$ and $J_2^{(i)}(2\omega)$ at 15.1 MHz, respectively, and the open and closed circles denote data at 46 MHz. Typical error bars are shown only in (a) for C_1 and C_2.

required in the *N* phase of 8OCB. Even though our relaxation data could be better fitted with increasing ODF contributions, this has been discouraged on account of the fact that collective motions are slow and only effective in relaxing nuclear spin at low Larmor frequencies (below 1 MHz in most cases). We have, therefore, imposed a linear temperature dependence for the high-frequency cutoff ($\omega_c/2\pi = 30$ MHz at 350 K) such that its value decreases to 3 MHz just below the *N*-Sm*A* phase transition at 335 K. In this manner, the cutoff function $\mathfrak{I}(x) \rightarrow 0$ in the Sm*A* phase. We found that ODF's contribute about 3–4 % to $J_1^{(i)}(\omega)$ at 15.1 MHz and 335 K, and make zero contributions to $J_1^{(i)}(\omega)$ at lower temperatures. At the high end of the *N* phase (350 K), ODF's contribute to $J_1^{(i)}(\omega)$ between 24% and 32% at 15.1 MHz (about 7% at 46 MHz), as a result of the cutoff frequency being 30 MHz at this temperature. As in 6OCB, we believe the motional biaxiality is small and have chosen $D_x = D_y = D_\perp$. The spectral densities $J_1^{(i)}(\omega)$ and $J_2^{(i)}(2\omega)$ for carbon 1 to carbon 7 are calculated using Eqs. (9) and (10) and compared with their experimental values in a global target analysis [32]. This approach takes advantage of the fact that the target model parameters vary smoothly with temperature and at *N*-Sm*A* transition. To get some ideas on the temperature behaviors of model parameters $D_\perp$, $D_\parallel$, k_1, k_2, and k_3, individual target analyses (i.e., analyses of spectral densities at each temperature) were first carried out. We found that the rotational diffusion constants obeyed simple Arrhenius relations

$$D_\perp = D_\perp^0 \exp[-E_a^{D_\perp}/RT], \tag{19}$$

$$D_\parallel = D_\parallel^0 \exp[-E_a^{D_\parallel}/RT], \tag{20}$$

while the jump constant k_3 for three-bond motions was temperature insensitive, and the other jump constants showed weak temperature behaviors given by

$$k_i = k_i' + k_i''(T - T_{\min}), \tag{21}$$

where $i = 1$ or 2 and $T_{\min}$ is 320 K. The pre-exponentials $D_\perp^0$ and $D_\parallel^0$ and their corresponding activation energies $E_a^{D_\perp}$ and $E_a^{D_\parallel}$ are the global parameters. Similarly k_3, k_1', k_1'', k_2', and k_2'' are the remaining global parameters in our global target analysis. Instead of Eqs. (19) and (20), these were rewritten in terms of the activation energies and the diffusion constants $D_\perp'$ and $D_\parallel'$ at $T_{\min}$. Indeed k_3, k_2', k_1', $D_\perp'$, and $D_\parallel'$ were first obtained at 320 K by an individual target analysis. The ODF prefactor *A* in Eq. (6) was input and found best at 9.9×10^{-6} $s^{1/2}$, a value consistent with those found in other liquid crystals [37]. We note that *A* was chosen to be independent of temperature. Thus the temperature dependences of ODF contributions came through ω_c in the cutoff function for the ODF modes. Alternatively, one may fix ω_c while letting *A* to decrease with decreasing temperature. Again AMOEBA was used to minimize the mean-squared percent deviation (F). The fitting quality factor Q is defined as

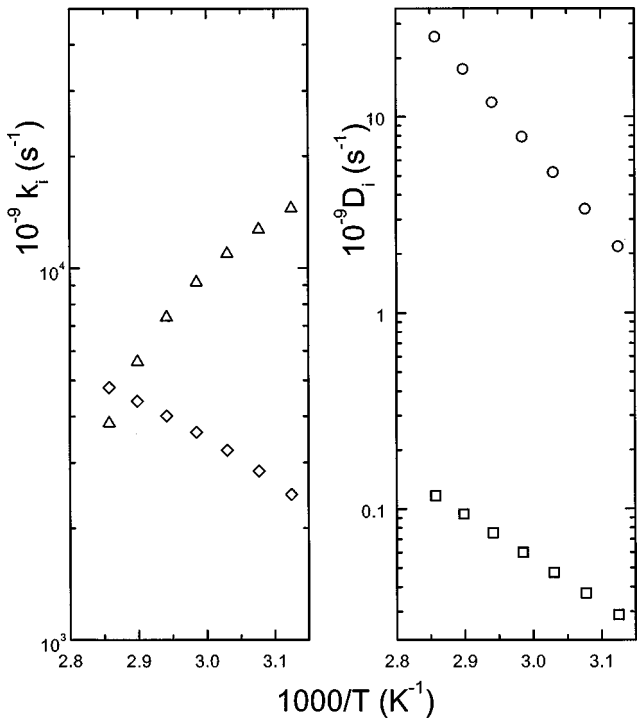

FIG. 6. Plots of jump rate constants k_1 (triangle) and k_2 (diamond), as well as rotational diffusion constants $D_\parallel$ (circle) and $D_\perp$ (square) as functions of the reciprocal temperature.

$$Q=\frac{\sum_k \sum_\omega \sum_i \sum_m [J_m^{(i)\mathrm{calc}}(m\omega)-J_m^{(i)\mathrm{expt}}(m\omega)]_k^2}{\sum_k \sum_\omega \sum_i \sum_m [J_m^{(i)\mathrm{expt}}(m\omega)]_k^2}, \tag{22}$$

where the sum over i covers C_1 to C_7 at 46 MHz and C_2 to C_7 at 15.1 MHz, the sum over ω is for two different Larmor frequencies, the sum over k is for seven temperatures, and $m=1$ and 2. The C_1 data at 15.1 MHz, as mentioned before, was not as reliable as others and hence was not included in F. We have a total of 172 spectral densities to derive nine global parameters. We found $Q=1.5\%$ and the calculated spectral densities (including C_1 at 15.1 MHz) are shown as solid $[J_1^{(i)}(\omega)]$ and dashed $[J_2^{(i)}(2\omega)]$ curves in Fig. 5. Although there are some systematic deviations between experimental and calculated spectral densities, the overall fits are quite satisfactory given the many simplifications (in particular the use of the ''pentane'' effect) in the motional model used in the present study. It is pleasing to note that the experimental $J_1^{(1)}(\omega)$ and $J_2^{(1)}(2\omega)$ were predicted rather well by our motional model. Now $k_3=9.8\times10^{16}$ s^{-1} for all temperatures, and other model parameters are summarized as plots shown in Fig. 6. The three-bond motions are very fast, and occur on a time scale of femtoseconds. Now k_2 decreases with increasing temperature, while k_1 shows an opposite temperature behavior. Similar temperature dependences for k_1 and k_2 were observed in 6OCB [9]. The activation energy $E_a^\parallel(=77.0$ kJ/mol) is higher than the activation energy $E_a^\perp(=43.4\pm1.3$ kJ/mol), which seems unphysical. This merely reflects the difficulty in obtaining information about the tumbling motion of the molecule, a phenomenon often encountered in NMR studies of liquid crystals [7,30,45]. The tumbling motion ($D_\perp$) is slow with a rate of the order of 5×10^7 s^{-1} and produces, therefore, some frequency dependences in both $J_1(\omega)$ and $J_2(2\omega)$. The error limit for a particular global parameter was estimated by varying the one under consideration while keeping all other global parameters identical to those for the minimum F, to give an approximate doubling in the F value. The error limits for $E_a^\parallel$ lie between 75.2 and 78.3 kJ/mol. In estimating the error limits for k_3, we found that any larger k_3 value does not affect the fits, and hence no upper limit can be estimated. Indeed there is a tendency in the minimization to overestimate the k_3 value. The lower error limit for k_3 is 2.5×10^{14} s^{-1}. To examine the error limits for k_1 and k_2 at $T_{\min}$ ($k_1'=1.45\times10^{13}$ s^{-1}, $k_2'=2.46\times10^{12}$ s^{-1}), we found $k_1'^{\uparrow}=2.55\times10^{13}$ s^{-1} and $k_1'^{\downarrow}=1.19\times10^{13}$ s^{-1}, while $k_2'^{\uparrow}=9\times10^{12}$ s^{-1} and $k_2'^{\downarrow}=6\times10^{11}$ s^{-1}, where the superscripts up and down arrows represent upper and lower error limits, respectively. The pre-exponentials in Eqs. (19) and (20) are $D_\perp^0=3.54\times10^{14}$ s^{-1} and $D_\parallel^0=7.95\times10^{21}$ s^{-1}. The error limits for $D_\perp^0$ lie between 2.25×10^{14} and 5.6×10^{14} s^{-1}, while for $D_\parallel^0$ they lie between 4.9×10^{21} and 1.5×10^{22} s^{-1}. Finally the correlation coefficients among various model parameters are addressed. The correlations between diffusion pre-exponentials and their corresponding activation energies are very high (near 1), and between k_1' and k_1'' the correlation is 0.95. The correlations between k_3 and all the diffusion parameters in Eqs. (19) and (20) and between k_1' and k_2' are 0.85. The correlation coefficients between other jump parameters are between 0.35 to 0.75, while the correlation coefficients between jump rate parameters (not k_3) and diffusion pre-exponentials (or activation energies) are between 0.2 and 0.5.

In summary, using the pentane effect to limit the number of conformations in 8OCB in calculating splittings and spectral densities appear to be a good approximation. Without it, the number of conformations would quadruple making the minimization too costly in computations. A consistent picture in interpretting both the splitting and relaxation data of 8OCB has emerged in the present study. In particular the decoupled model proposed by us has been successfully applied to a long-chain smectogen 8OCB, and the derived model parameters appear to be physically reasonable, except the low $E_a^\perp$ value. Application of the present methodology to other liquid crystals containing an octyloxy chain are currently in progress in our laboratory. The results will be communicated elsewhere.

ACKNOWLEDGMENTS

The financial support of the Natural Science and Engineering Council of Canada is gratefully acknowledged. We thank N. Finlay for his continuing technical assistance, Dr. G. M. Richards for her valuable contributions at the initial stage of this project, and M. Cheng for his assistance in some NMR experiments.

[1] R. Y. Dong, *Nuclear Magnetic Resonance of Liquid Crystals* (Springer-Verlag, New York 1997).
[2] S. Chandrasekhar, *Liquid Crystals* (Cambridge University Press, Cambridge, 1977); G. Vertogen and W. H. de Jeu, *Thermotropic Liquid Crystals, Fundamentals* (Springer-Verlag, Heidelberg, 1988).
[3] P. A. Beckmann, J. W. Emsley, G. R. Luckhurst, and D. L. Turner, Mol. Phys. **50**, 699 (1983); **59**, 97 (1986).
[4] R. Y. Dong and K. R. Sridharan, J. Chem. Phys. **82**, 4838 (1985).
[5] T. M. Barbara, R. R. Vold, R. L. Vold, and M. E. Neubert, J. Chem. Phys. **82**, 1612 (1985).
[6] D. Goldfarb, R. Y. Dong, Z. Luz, and H. Zimmermann, Mol. Phys. **54**, 1185 (1985).
[7] R. Y. Dong, L. Friesen, and G. M. Richards, Mol. Phys. **81**, 1017 (1994).
[8] L. Calucci, M. Geppi, C. A. Veracini, and R. Y. Dong, Chem. Phys. Lett. **296**, 357 (1998).
[9] X. Shen and R. Y. Dong, J. Chem. Phys. **108**, 9177 (1998).
[10] X. Shen, R. Y. Dong, N. Boden, R. J. Bushby, P. S. Martin, and A. Wood, J. Chem. Phys. **108**, 4324 (1998).
[11] A. Ferrarini, G. J. Moro, and P. L. Nordio, Liq. Cryst. **8**, 593 (1990).
[12] R. Y. Dong and G. M. Richards, Chem. Phys. Lett. **171**, 389 (1990).
[13] R. Y. Dong, Phys. Rev. A **43**, 4310 (1991).
[14] P. Pincus, Solid State Commun. **7**, 415 (1969).
[15] T. Lubensky, Phys. Rev. A **2**, 2497 (1970).
[16] J. W. Doane, C. E. Tarr, and M. A. Nickerson, Phys. Rev. Lett. **33**, 620 (1974).
[17] R. L. Vold, R. R. Vold, and M. Warner, J. Chem. Soc., Faraday Trans. II **84**, 997 (1988).
[18] G. van der Zwan and L. Plomp, Liq. Cryst. **4**, 133 (1989).
[19] M. Weger and B. Cabane, J. Phys. Colloq. **30**, C4-72 (1969).
[20] N. Bloembergen, E. M. Purcell, and R. V. Pound, Phys. Rev. **73**, 679 (1948).
[21] J. H. Freed, J. Chem. Phys. **66**, 4183 (1977).
[22] J. H. Freed, J. Chem. Phys. **41**, 2077 (1964); W. Huntress, Jr., Adv. Magn. Reson. **4**, 1 (1970).
[23] P. L. Nordio and P. Busolin, J. Chem. Phys. **55**, 5485 (1971); P. L. Nordio, G. Rigatti, and U. Segre, Mol. Phys. **25**, 129 (1973).
[24] J. M. Bernassau, E. P. Black, and D. M. Grant, J. Chem. Phys. **76**, 253 (1982).
[25] J. Bulthuis and L. Plomp, J. Phys. (Paris) **51**, 2581 (1990).
[26] R. Tarroni and C. Zannoni, J. Chem. Phys. **95**, 4550 (1991).
[27] E. Berggren, R. Tarroni, and C. Zannoni, J. Chem. Phys. **99**, 6180 (1993).
[28] E. Berggren and C. Zannoni, Mol. Phys. **85**, 299 (1995).
[29] P. J. Flory, *Statistical Mechanics of Chain Molecules* (Wiley, New York, 1969).
[30] R. Y. Dong and G. M. Richards, J. Chem. Soc., Faraday Trans. **88**, 1885 (1992).
[31] R. Y. Dong and G. M. Richards, Chem. Phys. Lett. **200**, 541 (1992).
[32] R. Y. Dong, Mol. Phys. **88**, 979 (1996).
[33] L. Calucci, C. Forte, M. Geppi, and C. A. Veracini, Z. Naturforsch. **53a**, 427 (1998).
[34] A. Arcioni, F. Bertinelli, R. Tarroni, and C. Zannoni, Chem. Phys. **143**, 259 (1990).
[35] J. P. Jacobsen, H. K. Bildsoe, and K. Schumburg, J. Magn. Reson. **23**, 153 (1976); S. B. Ahmad, K. J. Packer, and J. M. Ramsden, Mol. Phys. **33**, 857 (1977); R. R. Vold and R. L. Vold, J. Chem. Phys. **66**, 4018 (1977).
[36] C. J. R. Counsell, Ph.D. thesis, Southampton, 1983; C. J. R. Counsell, J. W. Emsley, G. R. Luckhurst, and H. S. Sachdev, Mol. Phys. **63**, 33 (1988).
[37] R. Y. Dong and X. Shen, J. Phys. Chem. A **101**, 4673 (1997).
[38] J. W. Emsley, G. R. Luckhurst, and C. P. Stockley, Proc. R. Soc. London, Ser. A **381**, 117 (1982).
[39] C. J. R. Counsell, J. W. Emsley, N. J. Heaton, and G. R. Luckhurst, Mol. Phys. **54**, 847 (1985).
[40] G. R. Luckhurst, C. Zannoni, P. L. Nordio, and U. Segre, Mol. Phys. **30**, 1345 (1975).
[41] J. W. Emsley, E. K. Foord, P. J. F. Gandy, and D. L. Turner, Liq. Cryst. **17**, 303 (1994).
[42] P. Diehl and W. Niederberger, J. Magn. Reson. **15**, 391 (1974).
[43] S. Wimperis, J. Magn. Reson. **83**, 590 (1990); **86**, 46 (1989).
[44] W. H. Press, B. P. Flannery, S. A. Teukolsky, and W. T. Vetterling, *Numerical Recipes* (Cambridge University Press, Cambridge, 1986).
[45] J. M. Goetz, G. L. Hoatson, and R. L. Vold, J. Chem. Phys. **97**, 1306 (1992).